FACTA UNIVERSITATIS
Series: **Electronics and Energetics** Vol. 37, Nº 2, June 2024, pp. 391 – 408
https://doi.org/10.2298/FUEE2402391S

Original scientific paper

CORRECTION OF THE IEC FORMULA FOR THE EDDY-CURRENT LOSS FACTOR: THE CASE OF SINGLE-CORE CABLES IN TREFOIL FORMATION WITH METALLIC SCREENS BONDED AND EARTHED AT ONE END

Marko Šućurović[1], Dardan Klimenta[2], Dragan Tasić[3]

[1]University of Kragujevac, Faculty of Technical Sciences,
Department of Power Engineering, Republic of Serbia
[2]University of Priština in Kosovska Mitrovica, Faculty of Technical Sciences,
Department of Power Engineering, Republic of Serbia
[3]University of Niš, Faculty of Electronic Engineering, Department of Power Engineering,
Republic of Serbia

ORCID iDs:	Marko Šućurović	https://orcid.org/0000-0001-9574-6101
	Dardan Klimenta	https://orcid.org/0000-0003-0019-8371
	Dragan Tasić	https://orcid.org/0000-0001-5957-9617

Abstract. *The purpose of this paper is to propose and apply the correct formula for the eddy-current loss factor for the case of three single-core cables in trefoil formation with metallic screens and armourings bonded and earthed at one end. This metallic screen bonding design is contrasted to the design where metallic screens and armourings are bonded and earthed at both ends, that is, the eddy-current loss factor is contrasted to the circulating-current loss factor. Ampacity calculations are carried out for 12 different underground lines with power cables of the type Cu/XLPE/CTS/PVC/AWA/PVC 1/C 19/33 kV (BS 6622), assuming that the 33 kV cables are installed directly in the soil without drying out. The ampacity is calculated analytically in accordance with IEC 60287-1-1 and IEC 60287-2-1, and numerically in accordance with IEC TR 62095. The numerical calculations are carried out to verify the accuracy of the proposed formula using the finite element method (FEM) in COMSOL 4.3. A validation of the proposed formula is conducted based on the manufacturer's technical data for the considered cables. The calculated ampacity values determined the incompleteness of the current IEC formula for the eddy-current loss factor, and verified the accuracy of the proposed one.*

Key words: *ampacity, circulating-current loss factor, eddy-current loss factor, finite element method (FEM), metallic screen bonding design, power cable*

Received January 09, 2024; revised February 21, 2024; accepted March 21, 2024
Corresponding author: Dardan Klimenta
University of Priština in Kosovska Mitrovica, Faculty of Technical Sciences, Department of Power Engineering, Republic of Serbia
E-mail: dardan.klimenta@pr.ac.rs

1. INTRODUCTION

The latest version of the IEC 60287-1-1 standard was published in May 2023 [1]. This standard retained the incomplete formula for the eddy-current loss factor for the case of three single-core cables in trefoil formation with screens and armourings from non-magnetic metals bonded and earthed at one end. Thus, this formula existed in the same form in earlier versions of the IEC 60287-1-1 standard. This formula has been causing difficulties for design-engineers when calculating the ampacity of underground cable lines for several decades and should be corrected adequately.

The current form of the formula for the eddy-current loss factor recommended by IEC 60287-1-1 [1] for three single-core cables in trefoil formation with metallic screens bonded and earthed at one end or cross-bonded is based on the researches conducted in earlier years [2-4]. The accuracy of the formulas for the calculation of metallic screen and armour losses in the 1994 version of the IEC 60287-1-1 standard was discussed by Barrett and Anders in 1997 [5]. Factors affecting metallic screen losses in underground cable lines with screens bonded and earthed at both ends were considered in [6]. In this regard, Anders also pointed out in 1997 [7] that eddy current losses occur regardless of the metallic screen bonding design, although they are often ignored in metallic screens bonded and earthed at both ends [1], where they are assumed to be small in magnitude compared to circulating current losses. For various metallic screen bonding designs and different short circuits, induced voltages and currents in metallic screens of high voltage underground cables in steady-state due to the adjacent cables and metallic screens were estimated in [8]. Formulas for the correction factor of three single-core cables with metallic screens cross-bonded and with unknown minor section lengths in order to correct the corresponding IEC 60287-1-1 formulas were provided in [9]. In addition, metallic screen voltages, circulating current losses, eddy current losses and associated loss factors for three single-core cables in trefoil and flat formations and various metallic screen bonding designs were simulated in [10].

Thermal and electrical effects of losses in metallic screens of single-core cables using the finite element method (FEM) were analyzed in [11]. Minimization of metallic screen and armour losses in an underground distribution network was performed in [12]. The paper [13] reviewed the formulas for induced losses in metallic screens used by IEC 60287-1-1 for cables in trefoil formation, making focus on three-core submarine cables with non-magnetic armourings. An improvement of loss allocation in three-core armoured cables using the FEM was proposed in [14]. The analytical techniques used to analyze currents and losses induced in armourings of medium voltage single-core cables were reviewed in [15]. Increasing the ampacity of underground cable lines by optimizing their crossings with respect to the metallic screen bonding designs was discussed in [16]. An improved analytical method for the cable ampacity calculation taking into account losses in metallic screens and armourings was proposed in [17]. Obviously, there have been attempts to correct or improve certain parts of the IEC 60287-1-1 standard that refer to losses due to eddy currents. However, the IEC formula for the eddy-current loss factor in question remained a research gap to be addressed in this paper.

According to the IEC 60287-1-1 standard [1], the eddy-current loss factor is the ratio of the losses due to eddy currents in one metallic screen per unit length to the losses in one conductor per unit length. In this paper, such an eddy-current loss factor is multiplied by the ratio of the effective cross-section of the conductor on one side and the sum of the effective cross-sections of the metallic screen and armouring on the other. The proposed

definition of the eddy-current loss factor can be regarded as the main contribution of this study. The idea for such a definition was found in [18], where losses due to eddy currents were included per unit volume. Ampacity calculations are performed for 12 different underground lines with power cables of the type Cu/XLPE/CTS/PVC/AWA/PVC 1/C 19/33 kV (BS 6622) from [19, 20], assuming that their metallic screens and armourings are bonded and earthed at both ends and at one end. These ampacity calculations are made in accordance with the IEC 60287-1-1 standard [1], the IEC 60287-2-1 standard [21] and the IEC TR 62095 technical report [22] using the FEM in COMSOL 4.3 [23].

2. Problem Formulation and Input Data

When the IEC 60287-1-1 standard is used to calculate the ampacities of power cables with metallic screens and armourings from non-magnetic materials, a problem is encountered with the application of the formula for estimating the eddy-current loss factor λ''_1. According to the IEC 60287-1-1 standard [1] from 2023, each non-magnetic metallic screen and its associated non-magnetic armouring are usually connected in parallel to form an enlarged metallic screen with a larger cross-section and lower electrical resistance per unit length. In this particular case, the corresponding IEC formula for the eddy-current loss factor λ''_1 does not provide a good estimate and should be adequately corrected.

The losses due to eddy currents in metallic screens of an underground cable line occur when the metallic screens are bonded and earthed at both ends [5,7,9,13] – to a low extent, as well as when the metallic screens are bonded and earthed at one end or cross-bonded [1] – to a significant extent. In the case of metallic screens bonded and earthed at both ends, the circulating currents counteract the magnetic field caused by the conductor current, and hence, affect the losses due to eddy currents. However, according to the 2023 version of the IEC 60287-1-1 standard [1], losses due to eddy currents should be ignored for the case of metallic screens bonded and earthed at both ends. Since the aforementioned incorrectness is analyzed, the neglect of eddy current losses in metallic screens bonded and earthed at both ends and other standardized assumptions must be used for the considered metallic screen bonding designs. The same assumptions are selected to compare the calculated results with those provided by the manufacturer in [19, 20]. Accordingly, the question is at which cross-section of the conductor the metallic screen bonding design [24] should be switched from the case of metallic screens bonded and earthed at both ends in accordance with Fig. 1(a) to the case of metallic screens bonded and earthed at one end in accordance with Fig. 1(b).

In order to obtain the correct formula for λ''_1, the following calculations for twelve different 33 kV underground lines with cables laid in trefoil formation will be performed: **(i)** ampacity calculations for cables with metallic screens and armourings bonded and earthed at both ends using the formula for the circulating-current loss factor λ'_1 from the IEC 60287-1-1 standard [1]; **(ii)** ampacity calculations for cables with metallic screens and armourings bonded and earthed at one end using the formula for the eddy-current loss factor λ''_1 from the IEC 60287-1-1 standard [1]; **(iii)** ampacity calculations for cables with metallic screens and armourings bonded and earthed at one end using a correct formula for the eddy-current loss factor λ''_1; and **(iv)** ampacity calculations for cables with metallic screens and armourings bonded and earthed at both ends and at one end using the FEM in the Heat Transfer Module of COMSOL 4.3 [23]. The results of the ampacity

calculations **(i)** will be used to identify the cross-sections of conductors for which incorrect or significantly high values of losses due to circulating currents in enlarged metallic screens occur. In addition, these results together with the results of the ampacity calculations **(iii)** will be used to respond to the question at which conductor cross-section the metallic screen bonding design should be switched from one case to another. The results of the ampacity calculations **(ii)** will be used to demonstrate the incorrectness of the formula for the eddy-current loss factor λ_1'' given in the IEC 60287-1-1 standard [1]. Numerical verification of the correctness of the current IEC formula for the circulating-current loss factor λ_1' and the proposed formula for the eddy-current loss factor λ_1'' will be conducted based on the results of the ampacity calculations **(iv)**.

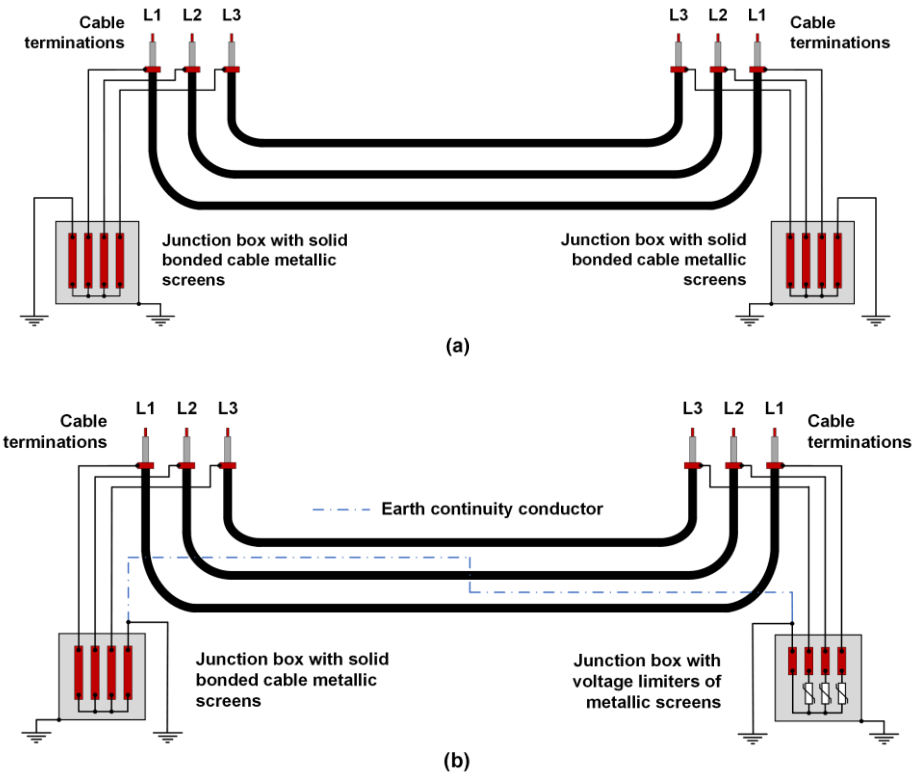

Fig. 1 A 33 kV underground cable line with (a) Metallic screens bonded and earthed at both ends; (b) Metallic screens bonded and earthed at one end

For the purpose of quantifying the effect of the conductor cross-section on the losses in metallic screens, the ampacity calculations will be carried out with 12 power cables of the type Cu/XLPE/CTS/PVC/AWA/PVC 1/C 19/33 kV (BS 6622) whose nominal cross-section $S_{C,n}$ ranges from 70 to 1000 mm^2. Service conditions as well as other constructional, electrical and rating data for these cables are taken directly from the manufacturer's technical documentation [19,20], or are estimated based on those data.

According to [19,20], the following service conditions are considered: three single-core cables installed directly in the soil, in trefoil formation, with metallic screens and armourings bonded and earthed at both ends or at one end; installation depth to center of trefoil formation L = 800 mm; referent soil temperature θ_{rs} = 15 °C; and thermal resistivity of the native soil $\rho_{t,s}$ = 1.2 K·m/W. Based on these conditions, it is evident that there is no drying out of the surrounding soil. The service conditions together with the details necessary for the FEM-based modeling (such as dimensions of the computational domain, boundary conditions, cable construction elements, etc.) are illustrated in Fig. 2.

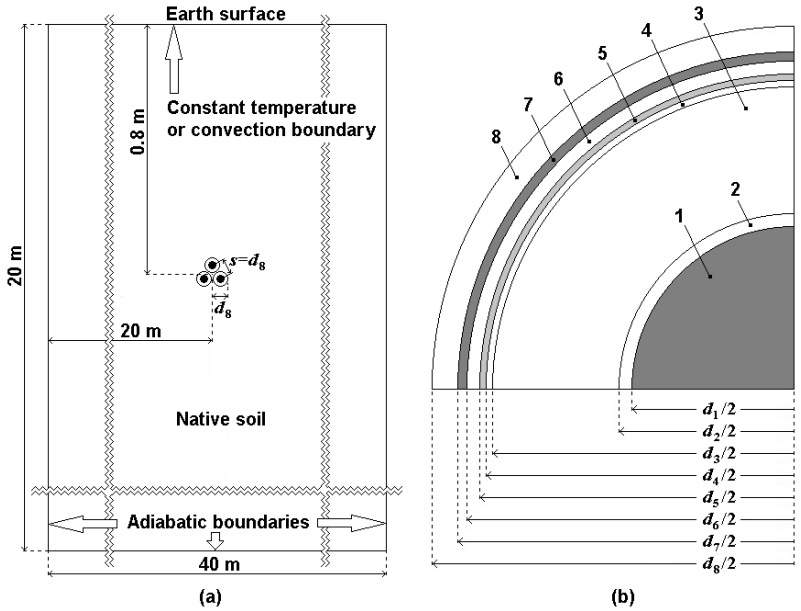

Fig. 2 Representation of the problem solved; (a) Computational domain referred to the design of a 33 kV underground cable line; (b) Dimensions of the construction elements of the Cu/XLPE/CTS/PVC/AWA/PVC 1/C 19/33 kV (BS 6622) cable, i.e., diameters of 1 – conductor, 2 – conductor screen, 3 – insulation, 4 – insulation screen, 5 – metallic screen, 6 – bedding, 7 – armouring, and 8 – oversheath

Data on cables with conductors of cross-sections from 50 to 630 mm^2 are given in [19], while data on cables with conductors of cross-sections from 70 to 1000 mm^2 are given in [20]. For conductors having cross-sections from 70 to 630 mm^2, the ampacity values from [19] are higher than those provided by the same manufacturer in [20]. In [19], for cables with 800 mm^2 and 1000 mm^2 conductor cross-sections, the following note is provided: “Please refer to our technical department for further information”. In addition to this, the service conditions are the same in [20] as they are in [19]. In this regard, the BS 6622:2007 standard [25] states the following: “In special circumstances it may be necessary to employ cross bonding or single-point bonding and in these cases recommendations should be sought from the manufacturer.” Therefore, in [20] it was certainly taken into account that metal screens and armourings of cables with 800 mm^2 and 1000 mm^2 conductor cross-

sections are bonded and earthed at one end. Based on this, the same assumption is accepted in this paper for cables with 800 mm^2 and 1000 mm^2 conductor cross-sections.

According to Fig. 2(a), s is the interaxial spacing between cables in trefoil formation in mm, and d_8 is the outer diameter of a cable in mm. Further, based on Fig. 2(b), d_1 is the diameter of a circular stranded copper conductor complying with IEC 60228 Class 2 [26] in mm; d_2 is the outer diameter of a conductor screen made of semi-conducting cross-linked polyethylene (XLPE) in mm; d_3 is the outer diameter of XLPE insulation in mm; d_4 is the outer diameter of a semi-conducting XLPE insulation screen in mm; d_5 is the outer diameter of a copper tape screen (CTS) in mm; d_6 is the outer diameter of polyvinyl chloride (PVC) bedding in mm; d_7 is the outer diameter of aluminium wire armouring (AWA) in mm, and d_8 is the outer diameter of a PVC oversheath (i.e., a cable) in mm. Table 1 outlines these diameters (d_i, i = 1,2,…8 in mm), maximum AC resistance of conductors at their continuously permissible temperature $\theta_{C,cp}$ = 90 °C per phase and unit length of a cable ($R_{C,l}$ in μΩ/m), and tabulated ampacity values ($I_{C,T}$ in A) for the 12 cables of the type Cu/XLPE/CTS/PVC/AWA/PVC 1/C 19/33 kV (BS 6622). The parameter $S_{s,n}$ appearing in Table 1 represents the nominal cross-section of a metallic screen in mm^2.

Table 1 Constructional, electrical and rating data on power cables of the type Cu/XLPE/CTS/PVC/AWA/PVC 1/C 19/33 kV (BS 6622)

$S_{C,n}/S_{s,n}$ (mm^2)/(mm^2)	d_1 (mm)	d_2 (mm)	d_3 (mm)	d_4 (mm)	d_5 (mm)	d_6 (mm)	d_7 (mm)	d_8 (mm)	$R_{C,l}$ (μΩ/m)	$I_{C,T}$ (A)
70/16	9.8	11	27	30.366	30.7	33.1	37.1	41.5	342	265
95/16	11.5	12.7	28.7	32.184	32.5	34.9	38.9	43.5	247	315
120/16	12.8	14	30	33.698	34	36.4	40.4	45	196	355
150/25	14.3	15.5	31.5	34.642	35.1	37.7	42.7	47.5	159	395
185/25	15.9	17.1	33.1	36.466	36.9	39.5	44.5	49.5	127	445
240/25	18.4	19.6	35.6	38.488	38.9	41.5	46.5	51.5	97.4	505
300/25	20.5	22.1	38.1	41.114	41.5	44.3	49.3	54.5	78.3	560
400/35	23.2	25.2	41.2	43.794	44.3	47.1	52.1	57.5	62.2	625
500/35	26.2	28.2	44.2	47.936	48.4	51.4	56.4	62	49.6	685
630/35	30.3	32.3	48.3	51.77	52.2	55.2	60.2	66	39.9	750
800/50	34.7	36.7	52.7	56.034	56.6	59.8	64.8	71	33.1	810
1000/50	38	41.3	57.3	60.172	60.7	64.1	69.1	75.5	28.4	855

Thermal, electrical and dielectric properties of materials used for IEC- and FEM-based modeling are shown in Table 2. The values for these material properties are taken from the standards IEC 60287-1-1 [1], IEC 60287-2-1 [21] and IEC 60287-3-1 [27], as well as from the available literature. The meanings of the parameters that appear in Table 2 are as follows: k_t is the thermal conductivity of the materials used in W/(K·m); ρ_e is the electrical resistivity of metallic screen or armouring material at the corresponding operating temperature in Ω·m; α_{20} is the temperature coefficient of electrical resistivity at 20 °C in 1/K; ε_r is the relative permittivity of the XLPE insulation; and tan δ is the loss factor for the XLPE insulation at a system frequency f = 50 Hz.

Table 2 Thermal, electrical and dielectric properties of materials used for modeling

Material	k_t [W/(K·m)]	ρ_e (Ω·m)	α_{20} (1/K)	ε_r (–)	$\tan\delta$ (–)
Aluminium at 20 °C	239	$2.84 \cdot 10^{-8}$	0.00403	–	–
Copper at 20 °C	385	$1.7241 \cdot 10^{-8}$	0.00393	–	–
XLPE	0.286	–	–	2.5	0.004
PVC	0.167	–	–	–	–
Native soil	0.83	–	–	–	–

3. IEC- AND FEM-BASED METHODS FOR CALCULATING THE CABLE AMPACITY

3.1. The current IEC 60287-based method

For three single-core cables installed directly in the soil without drying out, in trefoil formation, whose screens and armourings are made from non-magnetic metals, in parallel, bonded and earthed at both ends or at one end, the formula for the calculation of the cable ampacity I_C (in A) based on IEC 60287-1-1 and IEC 60287-2-1 reduces to [1,21,28]:

$$I_C = \left[\frac{\theta_{C,cp} - \theta_{rs} - W_{d,l}(0.5T_1 + T_2 + T_3 + T_4)}{R_{C,l}[T_1 + (1 + \lambda'_1 + \lambda''_1)(T_2 + T_3 + T_4)]} \right]^{0.5} \tag{1}$$

where $W_{d,l}$ represents the dielectric losses per phase and unit length of a cable in W/m, T_1 is the thermal resistance of the layers between one conductor and the corresponding metallic screen in K·m/W, T_2 is the thermal resistance of the PVC bedding in K·m/W, T_3 is the thermal resistance of the PVC oversheath in K·m/W, and T_4 is the thermal resistance of the surrounding soil in K·m/W. The remaining parameters appearing in Equation (1) are as follows: $R_{C,l}$ maximum AC resistance of one conductor at $\theta_{C,cp}$ = 90 °C in Ω/m (from Table 1), λ'_1 is the ratio of the losses due to circulating currents in one enlarged metallic screen to the losses in one conductor, and λ''_1 is the ratio of the losses due to eddy currents in one enlarged metallic screen to the losses in one conductor. According to the IEC 60287-1-1 standard [1], λ''_1 is equal to zero for metallic screens and armourings bonded and earthed at both ends, and λ'_1 is equal to zero for metallic screens and armourings bonded and earthed at one end (or cross-bonded).

For three single-core cables in trefoil formation with metallic screens and armourings bonded and earthed at both ends, the circulating-current loss factor λ'_1 is given by [1,28]:

$$\lambda'_1 = \frac{W_{se,l}}{W_{C,l}} = \frac{R_{se,l}}{R_{C,l}} \left[\frac{(2\pi f M)^2}{R_{se,l}^2 + (2\pi f M)^2} \right] \tag{2}$$

where $W_{se,l}$ represents the losses due to circulating currents in an enlarged metallic screen per phase and unit length of a cable in W/m, $W_{C,l}$ represents the losses in a conductor per phase and unit length of a cable in W/m, $R_{se,l}$ is the equivalent resistance of metallic screen and armouring in parallel in Ω/m, f = 50 Hz is the system frequency,

$$M = 2 \cdot 10^{-7} \ln\left(\frac{2s}{d_{se}}\right) \tag{3}$$

is the mutual inductance between a conductor and an enlarged metallic screen in H/m; and

$$d_{se} = \sqrt{\frac{(d_4 + d_5)^2 + (d_6 + d_7)^2}{8}} \tag{4}$$

is the mean diameter of an enlarged metallic screen in mm.

The AC resistance of any metallic screen at its maximum operating temperature $\theta_{s,\max}$ (in °C) per phase and unit length of a cable ($R_{s,l}$ in Ω/m) is calculated using an effective cross-section of the metallic screen $S_{s,eff} = \pi(d_5^2 - d_4^2) \cdot 10^{-6} / 4$ (in m^2). The maximum operating temperature $\theta_{s,\max}$ in °C is estimated by means of the following formula:

$$\theta_{s,\max} = \theta_{C,cp} - \frac{R_{C,l} I_{C,T}^2}{2\pi k_{t,XLPE}} \ln\left(\frac{d_4}{d_1}\right), \tag{5}$$

assuming $W_{d,l} = 0$ W/m for 33 kV cables.

The AC resistance of an armouring at its maximum operating temperature $\theta_{A,\max}$ (in °C) per phase and unit length of a cable ($R_{A,l}$ in Ω/m) is calculated using an effective cross-section of the armouring $S_{A,eff} = \pi(d_7^2 - d_6^2) \cdot 10^{-6} / 4$ (in m^2). The maximum operating temperature $\theta_{A,\max}$ in °C is estimated by means of the following formula:

$$\theta_{A,\max} = \theta_{C,cp} - \frac{R_{C,l} I_{C,T}^2}{2\pi}\left[\frac{1}{k_{t,XLPE}} \ln\left(\frac{d_4}{d_1}\right) + \frac{1}{k_{t,PVC}} \ln\left(\frac{d_6}{d_5}\right)\right], \tag{6}$$

assuming $W_{d,l} = 0$ W/m and $\lambda'_1 + \lambda''_1 = 0$ for 33 kV cables.

For three single-core cables in trefoil formation with metallic screens and armourings bonded and earthed at one end (or cross-bonded), the eddy-current loss factor λ''_1 is given by [1]:

$$\lambda''_1 = \frac{W_{se,l}}{W_{C,l}} = \frac{R_{se,l}}{R_{C,l}}\left[C_{gs}\lambda_0(1 + \Delta_1 + \Delta_2) + \frac{\beta_1^4 \Delta_{se}^4}{12 \cdot 10^{12}}\right] \tag{7}$$

where $W_{se,l}$ represents the losses due to eddy currents in an enlarged metallic screen per phase and unit length of a cable in W/m,

$$C_{gs} = 1 + \left(\frac{\Delta_{se}}{d_7}\right)^{1.74} (\beta_1 d_7 10^{-3} - 1.6), \tag{8}$$

$$\beta_1 = \sqrt{\frac{8\pi^2 f}{10^7 \rho_{se}}}, \tag{9}$$

$\rho_{se} = \dfrac{R_{s,l} S_{s,eff} R_{A,l} S_{A,eff}}{R_{s,l} S_{s,eff} + R_{A,l} S_{A,eff}}$ is the electrical resistivity of an enlarged metallic screen at its operating temperature in Ω·m, $\Delta_{se} = (d_7 - d_4)/2$ is the thickness of an enlarged metallic

screen in mm, and λ_0, C_{gs}, β_1, Δ_1 and Δ_2 are the appropriate coefficients. λ_0 is a dimensionless coefficient, C_{gs} is expressed in $[\text{m}\cdot\text{rad}/(\Omega\cdot\text{s})]^{0.5}$, β_1 is expressed in $[\text{rad}/(\Omega\cdot\text{m}\cdot\text{s})]^{0.5}$, while the units of the coefficients Δ_1 and Δ_2 can be obtained based on the given units.

Furthermore, for three single-core cables in trefoil formation is [1]:

$$m = \frac{2\pi f}{R_{s,l}} 10^{-7} \tag{10}$$

$$\lambda_0 = 3\left(\frac{m^2}{1+m^2}\right)\left(\frac{d_{se}}{2s}\right)^2 \tag{11}$$

where m is a parameter in $\text{m}\cdot\text{rad}/(\Omega\cdot\text{s})$,

$$\Delta_1 = (1.14m^{2.45} + 0.33)\left(\frac{d_{se}}{2s}\right)^{(0.92m+1.66)} \quad \text{and} \quad \Delta_2 = 0 \quad \text{for} \quad m > 0.1, \tag{12}$$

and

$$\Delta_1 = 0 \quad \text{and} \quad \Delta_2 = 0 \quad \text{for} \quad m \le 0.1. \tag{13}$$

3.2. A corrected IEC 60287-based method

Specifically, the corrected IEC-based method for the calculation of the cable ampacity I_C involves replacing Equation (7) with the following formula:

$$\lambda''_1 = \frac{S_{C,eff}}{S_{s,eff} + S_{A,eff}} \frac{R_{se,l}}{R_{C,l}} \left[C_{gs}\lambda_0(1+\Delta_1+\Delta_2) + \frac{\beta_1^4 \Delta_{se}^4}{12 \cdot 10^{12}} \right] \tag{14}$$

where $S_{C,eff} = \pi d_1^2 \cdot 10^{-6} / 4$ is the effective cross-section of a conductor in m^2. All other equations in this model are the same as in the IEC-based model from Section 3.1.

The ratio $S_{C,eff} / (S_{s,eff} + S_{A,eff})$ is found according to the ratio of the volume power of heat sources in one enlarged metallic screen $W_{se,v}$ (in W/m^3) to the volume power of heat sources in one conductor $W_{C,v}$ (in W/m^3) as follows:

$$\frac{W_{se,v}}{W_{C,v}} = \frac{W_{se,l} / (S_{s,eff} + S_{A,eff})}{W_{C,l} / S_{C,eff}} = \frac{S_{C,eff}}{S_{s,eff} + S_{A,eff}} \frac{W_{se,l}}{W_{C,l}} \tag{15}$$

where the term $W_{se,l} / W_{C,l}$ represents Equation (7) that comes from IEC 60287-1-1 [1].

3.3. The current IEC TR 62095-based method

Two-dimensional steady-state heat transfer through the computational domain in Fig. 2(a) is governed by the following second-order partial differential equation [29,30]:

$$\nabla \cdot (-k_t \nabla \theta) = \frac{\partial}{\partial x}\left(-k_t \frac{\partial \theta}{\partial x}\right) + \frac{\partial}{\partial y}\left(-k_t \frac{\partial \theta}{\partial y}\right) = W_v \tag{16}$$

where k_t is the thermal conductivity in $\text{W}/(\text{m}\cdot\text{K})$; θ is the unknown nodal temperature in K; x and y are the Cartesian spatial coordinates in m; and W_v is the volume power of heat sources in W/m^3.

For the purpose of thermal analysis using the FEM in COMSOL 4.3, any cable of the type Cu/XLPE/CTS/PVC/AWA/PVC 1/C 19/33 kV (BS 6622) needs to be represented by an equivalent construction consisted of the copper conductor, XLPE insulation, equivalent copper screen and PVC oversheath with outer diameters d_1, d_4, d_7 and d_8, respectively. The equivalent cable construction is based on the following IEC 60287-1-1 standard instruction [1]: "Where screening layers are present, for thermal calculations metallic tapes are considered to be part of the conductor or sheath while semi-conducting layers (including metallized carbon paper tapes) are considered as part of the insulation. The appropriate component dimensions must be modified accordingly." This means that the conductor and insulation screens are added to XLPE insulation, and materials of the copper screen, PVC bedding and aluminium armouring are modeled by the equivalent metallic screen having thermal conductivity of copper. Since the PVC bedding is included in the equivalent metallic screen, it means that the thermal resistance T_2 should be added to the thermal resistance T_3, that is, an equivalent thermal conductivity of the PVC oversheath should be determined. In that case, the equivalent thermal conductivity of the PVC oversheath $k'_{t,PVC}$ in W/(K·m) is

$$k'_{t,PVC} = \frac{1}{2\pi(T_2 + T_3)} \ln\left(\frac{d_8}{d_7}\right) \tag{17}$$

The volume power of heat sources in a conductor $W_{C,v}$ in W/m^3 is given by [29,30]:

$$W_{C,v} = \frac{W_{C,l}}{S_{C,eff}} = \frac{4R_{C,l}I_C^2}{\pi d_1^2 \cdot 10^{-6}} \tag{18}$$

where the cable ampacity I_C can be replaced with the tabulated ampacity value $I_{C,T}$, and the diameter d_1 is in mm.

The volume power of heat sources located between a conductor and an equivalent metallic screen $W_{d,v}$ in W/m^3 is given by [29, 30]:

$$W_{d,v} = \frac{4W_{d,l}}{\pi(d_4^2 - d_1^2) \cdot 10^{-6}} \tag{19}$$

where the diameters d_1 and d_4 are in mm.

The equivalent volume power of heat sources located between a semi-conducting XLPE insulation screen and a PVC oversheath $W'_{se,v}$ in W/m^3 is given by [29, 30]:

$$W'_{se,v} = \frac{4W_{se,l}}{\pi(d_7^2 - d_4^2) \cdot 10^{-6}} = \frac{4\lambda_1 W_{C,l}}{\pi(d_7^2 - d_4^2) \cdot 10^{-6}} = \frac{4\lambda_1 R_{C,l} I_C^2}{\pi(d_7^2 - d_4^2) \cdot 10^{-6}} \tag{20}$$

where the cable ampacity I_C can be replaced with the tabulated ampacity value $I_{C,T}$, $\lambda_1 = \lambda'_1$ for the case when enlarged metallic screens are bonded and earthed at both ends, $\lambda_1 = \lambda''_1$ for the case when enlarged metallic screens are bonded and earthed at one end, and the diameters d_4 and d_7 are in mm. The loss factor $\lambda_1 = \lambda'_1$ corresponds with Equation (2), while the loss factor $\lambda_1 = \lambda''_1$ corresponds with Equation (7) or Equation (14).

The top side of the computational domain in Fig. 2(a), i.e., the earth surface is modeled by

$$\theta = \theta_{rs} \tag{21}$$

– constant temperature boundary condition, or

$$\vec{n} \cdot (-k_t \nabla \theta) = h_c(\theta - \theta_{rs}) \tag{22}$$

– convection boundary condition [29,30]. In addition, the left-hand, bottom, and right-hand sides of the computational domain in Fig. 2(a) are modeled by

$$\vec{n} \cdot (-k_t \nabla \theta) = 0 \tag{23}$$

– adiabatic boundary condition [29,30]. In Equations (21-23), θ is the unknown temperature of the earth surface in K; θ_{rs} is the known temperature of the earth surface in K, or the known temperature of the air along the earth surface in K in accordance with IEC 60287-1-1 [1] and IEC TR 62095 [22]; $\vec{n}$ is the outwards-oriented normal vector of the constant temperature and convection boundaries; and h_c = 250 W/(m^2·K) is the heat transfer coefficient due to forced convection in accordance with IEC TR 62095 [22]. In addition, due to the absence of the radiation boundary condition, Equation (16) is linear.

4. Results and Discussion

The values of the thermal resistances and dielectric losses appearing in Equation (1) are listed in Table 3. In addition to these values Table 3 contains the equivalent thermal conductivity of the PVC oversheath calculated using Equation (17) for the purpose of FEM-based steady-state thermal modeling in COMSOL 4.3.

Table 3 Thermal resistances, equivalent thermal conductivity and dielectric losses for power cables of the type Cu/XLPE/CTS/PVC/AWA/PVC 1/C 19/33 kV (BS 6622)

$S_{C,n}/S_{s,n}$ (mm^2)/(mm^2)	T_1 (K·m/W)	T_2 (K·m/W)	T_3 (K·m/W)	T_4 (K·m/W)	$k'_{t,PVC}$ [W/(K·m)]	$W_{d,l}$ (W/m)
70/16	0.630	0.072	0.107	2.225	0.100	0.070556
95/16	0.573	0.068	0.107	2.198	0.102	0.077709
120/16	0.539	0.065	0.103	2.178	0.102	0.083128
150/25	0.493	0.068	0.102	2.147	0.100	0.089340
185/25	0.462	0.065	0.102	2.124	0.102	0.095927
240/25	0.411	0.062	0.097	2.101	0.102	0.106156
300/25	0.388	0.062	0.096	2.069	0.101	0.116326
400/35	0.354	0.058	0.094	2.038	0.103	0.128877
500/35	0.336	0.057	0.090	1.995	0.102	0.140977
630/35	0.298	0.053	0.088	1.959	0.104	0.157458
800/50	0.267	0.052	0.087	1.917	0.104	0.175093
1000/50	0.256	0.052	0.084	1.882	0.103	0.193488

Table 4 shows the circulating-current loss factor, volume powers of heat sources and maximum conductor temperatures obtained for the tabulated ampacity values and other service conditions taken from [20], and metallic screens and armourings bonded and earthed at both ends.

Based on the maximum conductor temperatures from the last two columns of Table 4 (which are higher than the continuously permissible temperature of 90 °C), it is obvious that there is something illogical about the cable ampacities provided by the manufacturer, or about the metallic screen bonding design. In particular, this means that the volume powers of heat sources in the conductors and equivalent metallic screens are not adequate and the reason for this should be identified. In this regard, the volume powers of heat sources in the XLPE insulations do not contribute to this illogicality.

Table 5 shows the circulating-current loss factor, volume powers of heat sources and maximum conductor temperatures obtained for the ampacities calculated in accordance with IEC 60287-1-1 [1], other service conditions taken from [19,20], and metallic screens and armourings bonded and earthed at both ends.

Table 4 Circulating-current loss factor, volume powers of heat sources and maximum conductor temperatures obtained for the tabulated ampacity values taken from [20], and metallic screens and armourings bonded and earthed at both ends

$S_{C,n}/S_{s,n}$	$I_{C,T}$	λ'_1	$W_{C,v}$	$W_{d,v}$	$W'_{se,v}$	$\theta_{C,\max}$*	$\theta_{C,\max}$**
(mm²)/(mm²)	(A)	(–)	(W/m³)	(W/m³)	(W/m³)	(°C)	(°C)
70/16	265	0.060335	318402.0	147.7	4061.0	91.495	91.556
95/16	315	0.084997	235956.8	149.4	5555.9	92.390	92.453
120/16	355	0.107885	191956.5	150.3	6832.4	92.758	92.823
150/25	395	0.161023	154464.7	151.3	8161.0	94.222	94.290
185/25	445	0.203234	126660.0	152.1	10004.5	96.181	96.253
240/25	505	0.265159	93414.9	153.0	12315.7	96.472	96.547
300/25	560	0.333637	74394.4	153.8	14093.4	97.678	97.756
400/35	625	0.428533	57475.7	154.4	16644.1	99.838	99.921
500/35	685	0.540382	43168.8	154.9	18132.8	99.751	99.953
630/35	750	0.672362	31125.8	155.5	20355.4	100.645	100.734
800/50	810	0.820678	22964.1	155.8	21423.5	102.309	102.403
1000/50	855	0.953514	18306.0	156.1	21838.8	102.380	102.477

* Values obtained using the FEM in COMSOL 4.3 for the earth surface represented by the constant temperature boundary condition.
** Values obtained using the FEM in COMSOL 4.3 for the earth surface represented by the convection boundary condition.

Table 5 Circulating-current loss factor, volume powers of heat sources and maximum conductor temperatures obtained for the ampacities calculated in accordance with IEC 60287-1-1 [1], and metallic screens and armourings bonded and earthed at both ends

$S_{C,n}/S_{s,n}$	I_C	λ'_1	$W_{C,v}$	$W_{d,v}$	$W'_{se,v}$	$\theta_{C,\max}$*	$\theta_{C,\max}$**
(mm²)/(mm²)	(A)	(–)	(W/m³)	(W/m³)	(W/m³)	(°C)	(°C)
70/16	262.321	0.060334	311997.9	147.7	3979.3	89.962	90.021
95/16	310.168	0.084997	228772.7	149.4	5386.7	89.042	90.103
120/16	348.664	0.107885	185145.0	150.3	6589.9	90.009	90.072
150/25	384.343	0.161023	146242.3	151.3	7726.6	90.021	90.086
185/25	427.668	0.203234	116985.7	152.1	9240.4	90.005	90.071
240/25	484.349	0.265159	85931.2	153.0	11329.1	89.972	90.041
300/25	533.130	0.333637	67426.5	153.8	12773.4	89.969	90.040
400/35	587.154	0.428533	50725.7	154.4	14689.4	89.921	89.994
500/35	643.392	0.540382	38083.9	154.9	15996.9	89.924	89.999
630/35	700.680	0.672362	27166.7	155.5	17766.3	89.813	89.891
800/50	749.603	0.820678	19667.2	155.8	18347.8	89.849	89.930
1000/50	790.828	0.953514	15661.2	156.1	18683.6	89.838	89.921

* Values obtained using the FEM in COMSOL 4.3 for the earth surface represented by the constant temperature boundary condition.
** Values obtained using the FEM in COMSOL 4.3 for the earth surface represented by the convection boundary condition.

From Table 5, it is evident that the maximum conductor temperatures are approximately equal to the continuously permissible temperature of 90 °C. Thus, the IEC-based ampacity calculation was carried out correctly. In addition, it is found that the cable ampacity values are lower than those given by the manufacturer in [20] and that the circulating-current loss factors remained unchanged. Consequently, it remains that the cable ampacity values from [20] were not obtained in accordance with IEC 60287-1-1 [1], or that, at some conductor cross-section, the metallic screen bonding design was switched from the case shown in Fig. 1(a) to that of Fig. 1(b).

Table 6 outlines the eddy-current loss factor, volume powers of heat sources and maximum conductor temperatures obtained for the ampacities calculated in accordance with IEC 60287-1-1 [1] using the current IEC formula for λ''_1, other service conditions taken from [19,20], and metallic screens and armourings bonded and earthed at one end.

Table 6 Eddy-current loss factor, volume powers of heat sources and maximum conductor temperatures obtained for the ampacities calculated in accordance with IEC 60287-1-1 [1] using the current IEC formula for λ''_1, and metallic screens and armourings bonded and earthed at one end

$S_{C,n}/S_{s,n}$	I_C	λ''_1	$W_{C,v}$	$W_{d,v}$	$W'_{se,v}$	$\theta_{C,\max}$*	$\theta_{C,\max}$**
(mm²)/(mm²)	(A)	(–)	(W/m³)	(W/m³)	(W/m³)	(°C)	(°C)
70/16	266.978	0.014608	323172.7	147.7	997.9	89.953	90.012
95/16	317.977	0.020635	240437.8	149.4	1374.4	90.036	90.096
120/16	359.743	0.026621	197120.0	150.3	1731.2	90.006	90.068
150/25	401.872	0.043799	159886.0	151.3	2297.8	90.013	90.077
185/25	452.068	0.055645	130715.8	152.1	2826.9	89.992	90.058
240/25	519.872	0.074165	98998.0	153.0	3650.6	89.958	90.026
300/25	580.642	0.096986	79980.1	153.8	4404.4	89.972	90.041
400/35	651.733	0.129025	62497.7	154.4	5449.2	89.930	90.001
500/35	727.254	0.171481	48658.8	154.9	6485.9	89.932	90.006
630/35	808.811	0.219644	36198.6	155.5	7733.3	89.836	89.912
800/50	879.755	0.286259	27089.6	155.8	8815.2	89.865	89.943
1000/50	939.099	0.348455	22084.3	156.1	9628.1	89.859	89.940

* Values obtained using the FEM in COMSOL 4.3 for the earth surface represented by the constant temperature boundary condition.
** Values obtained using the FEM in COMSOL 4.3 for the earth surface represented by the convection boundary condition.

Based on Table 6, the maximum conductor temperatures are close to the continuously permissible temperature of 90 °C. It seems that the ampacity calculations were carried out as required by the IEC 60287-1-1 standard. However, for conductor cross-sections equal to or larger than 400 mm², it is found that the ampacities are significantly higher than those provided by the manufacturer in [20]. In addition, all the values of the eddy-current loss factor are lower than 0.35. The eddy-current loss factors are significantly lower than the corresponding circulating-current loss factors. Thus, the metallic screens and armourings for all conductor cross-sections had to be bonded and earthed at one end instead of both. This does not agree with the service conditions given in [20] and indicates that something is wrong with the current IEC formula for the eddy-current loss factor. It also follows that the ampacities provided by the manufacturer in Table 4 for all conductor cross-sections are obtained as approximate mean values of the ampacities from

Tables 5 and 6 (corresponding to the two considered bonding designs). Such approach also does not agree with the guidelines of IEC 60287-1-1 [1].

Furthermore, when comparing the ampacities of cables having conductor cross-sections of 800 mm^2 and 1000 mm^2 from Table 4 to the corresponding ampacities from Tables 5 and 6, it is noticed that the ampacities of 810 A and 855 A are significantly higher than those of Table 5, and significantly less than those of Table 6. If it is taken into account that Equation (2) is correct, then it follows that the error occurs when applying Equation (7). This was an alternative way to show that the ampacities of 810 A and 855 A correspond to the case of cables with metallic screens and armourings bonded and earthed at one end. Thus, the given data can be used to validate the accuracy of the proposed formula for eddy-current loss factor, that is, Equation (14).

The validation process consists of the following five steps: **(i)** In the FEM-based steady-state thermal model used to generate the corresponding results from Table 4, it should be specified $W'_{se,v}$=0 W/m^3, while all other parameters remain the same. **(ii)** The value of the equivalent volume power of heat sources located in the equivalent metallic screen $W'_{se,v}$ needs to be increased from simulation to simulation until a value corresponding to the continuously permissible temperature of 90 °C is identified. **(iii)** The losses due to eddy currents in an enlarged metallic screen per phase and unit length of a cable $W_{se,l}$ need to be calculated using Equation (20). **(iv)** The losses in a conductor per phase and unit length of a cable $W_{C,l}$ need to be calculated using Equation (18). **(v)** The eddy-current loss factor needs to be calculated as $\lambda''_1 = W_{se,l} \,.\, W_{C,l}$. The results of this validation process are shown in Table 7 and Fig. 3.

Table 7 Volume powers of heat sources, maximum conductor temperatures and eddy-current loss factor obtained for the tabulated ampacity values taken from [20], and metallic screens and armourings bonded and earthed at one end

$S_{C,n}/S_{s,n}$	$I_{C,T}$	$W_{C,v}$	$W_{d,v}$	$W'_{se,v}$	$\theta_{C,\max}$ *	$\theta_{C,\max}$ **	λ''_1 ***
(mm^2)/(mm^2)	(A)	(W/m^3)	(W/m^3)	(W/m^3)	(°C)	(°C)	(–)
800/50	810	22964.1	155.8	14198.3	90.000	90.080	0.543899
1000/50	855	18306.0	156.1	15039.1	90.000	90.082	0.656629

* Values obtained using the FEM in COMSOL 4.3 for the earth surface represented by the constant temperature boundary condition

** Values obtained using the FEM in COMSOL 4.3 for the earth surface represented by the convection boundary condition

*** Values obtained using Equations (18) and (20) in combination with the following definition:

$$\lambda''_1 = W_{se,l} / W_{C,l}$$

According to Tables 6 and 7, each eddy-current loss factor from Table 7 is approximately twice as large as the corresponding loss factor from Table 6. The ratio between the eddy-current loss factors from Tables 7 and 6 is obviously comparable to the cross-section ratio $S_{C,eff} / (S_{s,eff} + S_{A,eff})$ that appears in Equation (14). It can therefore be considered that, in this manner, the accuracy of Equation (14) is validated. In addition, temperature distributions over the part of the computational domain in Fig. 2(a) generated using the data from Table 7 for the considered cables with 800 mm^2 and 1000 mm^2 conductor cross-sections are shown in Figs. 3(a) and 3(b), respectively. These two temperature distributions correspond with the cases where the equivalent metallic screen has the thermal conductivity of copper and where the earth surface is represented by the

constant temperature boundary condition. In order to show how the temperature distributions could be affected by the assumption that the equivalent metallic screens are made of aluminium instead of copper, two additional simulations were performed. The results of these additional simulations are shown in Figs. 3(c) and 3(d).

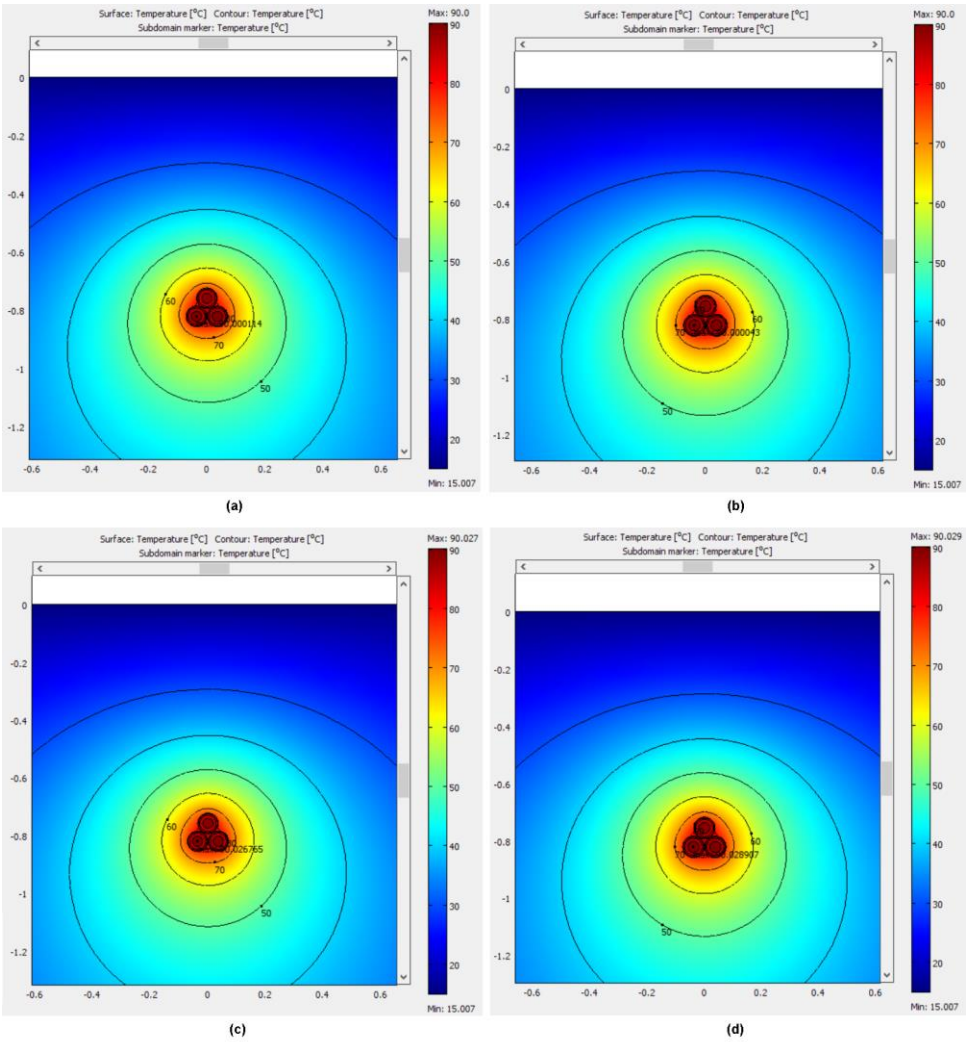

Fig. 3 Temperature distributions over the part of the computational domain in Fig. 2(a) generated using the data from Table 7 for the Cu/XLPE/CTS/PVC/AWA/PVC 1/C 19/33 kV (BS 6622) power cables with (a) 800 mm^2 conductor cross-section and equivalent copper screen; (b) 1000 mm^2 conductor cross-section and equivalent copper screen; (c) 800 mm^2 conductor cross-section and equivalent aluminium screen; (d) 1000 mm^2 conductor cross-section and equivalent aluminium screen

According to Figs. 3(a) and 3(c), as well as Figs. 3(b) and 3(d), the assumption that the equivalent metallic screens are made of aluminium instead of copper would lead to increases in the temperatures of the conductors by approximately 0.03 °C. Accordingly, it follows that the assumption used for equivalent metallic screens is justified by these comparisons. Furthermore, there is no need to show additional temperature distributions because of their similarity with those of Fig. 3.

Table 8 outlines the eddy-current loss factor, volume powers of heat sources and maximum conductor temperatures obtained for the ampacities calculated in accordance with IEC 60287-1-1 [1] using the correct formula for λ''_1, other service conditions taken from [19,20], and metallic screens and armourings bonded and earthed at one end.

Table 8 Eddy-current loss factor, volume powers of heat sources and maximum conductor temperatures obtained for the ampacities calculated in accordance with IEC 60287-1-1 [1] using the correct formula for λ''_1, and metallic screens and armourings bonded and earthed at one end

$S_{C,n}/S_{s,n}$	I_C	λ''_1	$W_{C,v}$	$W_{d,v}$	$W_{se,v}$	$\theta_{C,\max}$*	$\theta_{C,\max}$**
(mm²)/(mm²)	(A)	(–)	(W/m³)	(W/m³)	(W/m³)	(°C)	(°C)
70/16	268.024	0.004658	325711.1	147.7	320.7	89.951	90.010
95/16	319.498	0.008646	242743.5	149.4	581.4	90.034	90.095
120/16	361.663	0.013312	199230.4	150.3	875.0	90.005	90.067
150/25	405.628	0.020640	162888.4	151.3	1103.1	90.011	90.075
185/25	456.540	0.031134	133314.3	152.1	1613.1	89.990	90.055
240/25	524.264	0.053211	100677.6	153.0	2663.6	89.957	90.024
300/25	584.204	0.081535	80964.3	153.8	3748.3	89.972	90.041
400/35	651.874	0.128467	62524.7	154.4	5428.0	89.930	90.001
500/35	719.131	0.201665	47577.9	154.9	7458.1	89.932	90.005
630/35	779.400	0.324354	33613.8	155.5	10604.6	89.829	89.906
800/50	819.562	0.501903	23509.5	155.8	13413.1	89.858	89.938
1000/50	846.368	0.689442	17938.2	156.1	15473.4	89.846	89.928

* Values obtained using the FEM in COMSOL 4.3 for the earth surface represented by the constant temperature boundary condition.
** Values obtained using the FEM in COMSOL 4.3 for the earth surface represented by the convection boundary condition.

According to Table 8, it is clear that the maximum conductor temperatures are again close to 90 °C. This means that the IEC-based ampacity calculation using the correct formula for λ''_1 was carried out properly. Except for the case of a conductor cross-section of 1000 mm², it is obtained that the ampacities are higher than those provided by the manufacturer in [20] (Table 4), and that the eddy-current loss factors are lower than the corresponding circulating-current loss factors. Again, on the basis of Tables 4, 5 and 8, it follows that the ampacities of the manufacturer for conductor cross-sections from 70 mm² to 630 mm² are obtained as approximate mean values of the ampacities from Tables 5 and 8. As in previous discussion, the results again confirmed that the ampacities of the manufacturer (from Table 4) related to 800 mm² and 1000 mm² conductor cross-sections correspond with the case where metallic screens and armourings are bonded and earthed at one end in accordance with Fig. 1(b).

5. CONCLUSION

Based on the obtained results and their discussion, the following conclusions are reached: (**i**) It was shown that the ampacities obtained using the proposed formula for the eddy-current loss factor are closer to the tabulated ampacities provided by the manufacturer than those obtained using the current IEC formula. (**ii**) It was also shown that the tabulated ampacities provided by the manufacturer do not correspond with the design according to which metallic screens and armourings are bonded and earthed at both ends. (**iii**) It was found that the manufacturer switched from the case of metallic screens and armourings bonded and earthed at both ends to the case of metallic screens and armourings bonded and earthed at one end for conductor cross-sections of 800 mm^2 and 1000 mm^2, where the circulating-current loss factor is higher than 0.8. (**iv**) For conductor cross-sections of 800 mm^2 and 1000 mm^2, it was shown that the current IEC formula gives approximately half the value of that obtained by applying the correct formula.

Finally, FEM-based calculations of the circulating- and eddy-current loss factors for underground power cables with metallic screens and armourings bonded and earthed at both ends, using the IEC 60287-1-1 standard and assuming non-uniform current densities across the cross-sections of conductors, metallic screens and armourings, might be the subject of a future study. These numerical calculations should be performed assuming that three single-core cables are installed in trefoil formation and directly in the soil without drying out.

Acknowledgement: *This paper is a part of the research conducted within the projects No. NIO 200132, NIO 200155 and NIO 200148 supported by the Ministry of Education, Science and Technological Development of the Republic of Serbia*.

REFERENCES

[1] Electric cables – Calculation of the current rating – Part 1-1: Current rating equations (100% load factor) and calculation of losses – General. *IEC 60287-1-1:2023 CMV*, Ed. 3.0, 2023.

[2] P. G. Heyda, G. E. Kitchie and J. E. Taylor, "Computation of eddy-current losses in cable sheaths and busbar enclosures", *Proc. Inst. Electr. Eng.*, vol. 120, no. 4, pp. 447-452, April 1973.

[3] R. L. Jackson, "Eddy-current losses in unbounded tubes", *Proc. Inst. Electr. Eng.*, vol. 122, no. 5, pp. 551–557, May 1975.

[4] E. Kuffel and J. Poltz, "AC losses in crossbonded and bonded at both ends high voltage cables", *IEEE Trans. Power Appar. Syst.*, vol. PAS-100, no. 1, pp. 369–374, January 1981.

[5] J. S. Barrett and G. J. Anders, "Circulating current and hysteresis losses in screens, sheaths and armour of electric power cables – mathematical models and comparison with IEC Standard 287", *IEE Proc. – Sci. Meas. Technol.*, vol. 144, no. 3, pp. 101–110, May 1997.

[6] O. E. Gouda and A. E. E. Farag, "Factors affecting the sheath losses in single-core underground power cables with two-points bonding method", *Int. J. Electr. Comput. Eng.*, vol. 2, no. 1, pp. 7–16, February 2012.

[7] G. J. Anders. *Rating of Electric Power Cables: Ampacity Computations for Transmission, Distribution, and Industrial Applications*. New York: McGraw-Hill Professional and IEEE Press, 1997.

[8] M. Santos and M. A. Calafat, "Dynamic simulation of induced voltages in high voltage cable sheaths: Steady state approach", *Int. J. Electr. Power Energy Syst.*, vol. 105, pp. 1–16, February 2019.

[9] S. M. Noufal and G. J. Anders, "Sheath losses correction factor for cross-bonded cable systems with unknown minor section lengths: Analytical expressions", *IET Gener. Transm. Distrib.*, vol. 15, no. 5, pp. 849–859, March 2021.

[10] M. N. Abed, O. A. Suhry and M. A. Ibrahim, "Simulation of sheath voltage, losses and loss factor of high voltage underground cable using MATLAB/Simulink", *Int. J. Power Electron. Drive Syst.*, vol. 13, no. 1, pp. 220–215, March 2022.

[11] M. Rasoulpoor, M. Mirzaie and S. M. Mirimani, "Electrical and thermal analysis of single conductor power cable considering the lead sheath effect based on finite element method", *Iran. J. Electr. Electron. Eng.*, vol. 12, no. 1, pp. 73–81, March 2016.
[12] A. Ariyasinghe, C. Warnakulasuriya, S. Kumara and M. Fernando, "Optimizing medium voltage underground distribution network with minimized sheath and armor losses", In Proceedings of the 14th Conference on Industrial and Information Systems (ICIIS). Kandy, Sri Lanka: IEEE, 2019, pp. 119–124.
[13] D. Chatzipetros and J. A. Pilgrim, "Impact of proximity effects on sheath losses in trefoil cable arrangements", *IEEE Trans. Power Deliv.*, vol. 35, no. 2, pp. 455–463, April 2020.
[14] J. C. del-Pino-López and P. Cruz-Romero, "Use of 3D-FEM tools to improve loss allocation in three-core armored cables", *Energies*, vol. 14, no. 9, p. 2434, April 2021.
[15] P. Zamani, A. Foomezhi and S. G. Nohooji, "A review of medium voltage single-core cable armouring, induced currents and losses" *Energy Power Eng.*, vol. 13, no. 7, pp. 272–292, July 2021.
[16] B. Perović, D. Klimenta, D. Tasić, N. Raičević, M. Milovanović, M. Tomović and J. Vukašinović, "Increasing the ampacity of underground cable lines by optimising the thermal environment and design parameters for cable crossings", *IET Gener. Transm. Distrib.*, vol. 16, no. 11, pp. 2309–2318, June 2022.
[17] T. Szczegielniak, P. Jabłoński and D. Kusiak, "Analytical approach to current rating of three-phase power cable with round conductors", *Energies*, vol. 16, no. 4, p. 1821, February 2023.
[18] G. Aubert, J.-F. Jacquinot and D. Sakellariou, "Eddy current effects in plain and hollow cylinders spinning inside homogeneous magnetic fields: Application to magnetic resonance", *J. Chem. Phys.*, vol. 137, p. 154201, October 2012.
[19] Standard MV power cables – BS6622/BS7835 single core armoured 33 kV XLPE stranded copper conductor. Feb. 17, 2024. Available at: https://www.cablejoints.co.uk/upload/33kV_Single_Core__XLPE_AWA_Stranded_Copper_Conductor_HV_Cable.pdf.
[20] Standard MV power cables – BS6622/BS7835 single core armoured 33 kV XLPE stranded copper conductor. Dec. 31, 2023. Available at: https://www.powerandcables.com/wp-content/uploads/2017/03/33kV-MV-Cables-BS6622-BS7835-Single-Core-XLPE-AWA-Stranded-Copper-Conductors.pdf.
[21] Electric cables – Calculation of the current rating – Part 2-1: Thermal resistance – Calculation of the thermal resistance. *IEC 60287-2-1:2023 CMV*, Ed. 3.0, 2023.
[22] Electric cables – Calculations for current ratings – Finite element method. *IEC TR 62095:2003*, Ed. 1.0, 2003.
[23] Heat transfer module user's guide. COMSOL Inc., Version 4.3, 2012.
[24] Application note 3.1 – Cable sheaths – Overvoltage protection. Dec. 31, 2023. Available at: https://library.e.abb.com/public/42ff93fa18234d5982dad9bfc38482b7/ABB_AppNotes_3.1_Cable%20sheaths%20overvoltage%20protection%201HC0138880%20EN%20AA.pdf?x-sign=GeI5dghuY/Ig/vL9TLJsm1/UdXVxiljfhZeY1f3k+41SzISTBP+ntPkLSoppBhPH.
[25] Electric cables – Armoured cables with thermosetting insulation for rated voltages from 3.8/6.6 kV to 19/33 kV – Requirements and test methods. *BS 6622:2007*, Ed. 4.0, 2007.
[26] Conductors of insulated cables. *IEC 60228:2023 CMV*, Ed. 4.0, 2023.
[27] Electric cables – Calculation of the current rating – Part 3-1: Operating conditions – Site reference conditions. *IEC 60287-3-1:2017 RLV*, Ed. 2.0, 2017.
[28] L. Heinhold. *Power Cables and Their Application-Part 1*. Berlin: Siemens Aktiengesellschaft, 1990.
[29] M. Stojanović, J. Klimenta, M. Panić, D. Klimenta, D. Tasić, M. Milovanović and B. Perović, "Thermal aging management of underground power cables in electricity distribution networks: a FEM-based Arrhenius analysis of the hot spot effect", *Electr. Eng.*, vol. 105, pp. 647–662, 2023.
[30] D. Klimenta, B. Perović, J. Klimenta, M. Jevtić, M. Milovanović and I. Krstić, "Controlling the thermal environment of underground cable lines using the pavement surface radiation properties", *IET Gener. Transm. Distrib.*, vol. 12, no. 12, pp. 2968–2976, May 2018.